Finite-element analysis of the effect of sheath-gas composition in an inductively-coupled plasma

IOP Conf. Series: Materials Science and Engineering **430** (2018) 012024 doi:10.1088/1757-899X/430/1/012024

Finite-element analysis of the effect of sheath-gas composition in an inductively-coupled plasma

N J M Grobler[1,*], H Bissett[2], G J Puts[1], P L Crouse[1]

[1] Department of Chemical Engineering, University of Pretoria, Private Bag X20, Hatfield 0028, South Africa
[2] Division of Applied Chemistry, Nuclear Energy Corporation of South Africa, R104 Pelindaba, Madibeng 0240, South Africa

[*]njmgrobler@gmail.com

Abstract. The sheath gas plays an important role in inductively-coupled plasmas (ICPs) in preventing thermal damage to the side wall of the torch. The sheath gas (hydrogen in our case) is more difficult to ionise than argon (the main plasma gas) due to its lower electrical conductivity at the working temperature, preventing plasma formation and concomitant high temperatures in the immediate vicinity of the torch inside wall. The sheath gas also has a higher flow rate, reducing the time for heat transfer from the plasma to the inside wall. Numerous models to simulate an ICP reactor have been published in the open literature, none of which take into account the effect of characteristics of the sheath gas on the performance of an ICP on the heat transfer from the plasma to the sidewall of the reactor. The H_2:Ar gas ratio can have severely detrimental effects on the efficiency of the plasma because of the higher ionisation potential of H_2. Excess hydrogen in the sheath gas may also constitute material wastefulness. Both of these factors have an implication on the economics of the plasma process. This research aims at finding the optimum sheath-gas flow for the Necsa torch, used for spheroidisation. The work was done on the commercial finite-element programme COMSOL Multiphysics.

1. Introduction

Inductively coupled plasma (ICP) torches find application in a number of industrial settings, including the preparation of metal powders for additive manufacturing [1]. Spheroidised metal particles exhibit a uniform particle morphology and this uniformity imparts superior processing characteristics to the metal powders. The Nuclear Energy Corporation of South Africa (Necsa) has embarked on a program of spheroidisation technology development, with the ultimate aim of creating a commercial plasma-based metals processing facility. The developmental research is being conducted on a Tekna TEKSPHERO-15 [2] small-scale spheroidisation system using argon as operating gas. This system (and all other ICP plasma systems) suffers from energy efficiency issues. The plasma torch loses large amounts of energy to the water cooling in the torch sidewall. Successful commercialization of the technology requires mitigation of this energy loss.

The energy lost through the sidewall can be reduced by moving the plasma heated zone away from the sidewall. This may be effected by isolating the sidewall with a sheath gas that is more difficult to ionize than the operating gas. Hydrogen is more difficult to ionize than argon, therefore introducing hydrogen into the sheath gas moves the heated zone away from the torch sidewalls. Excess hydrogen can, however, be detrimental to the plasma, extinguish the plasma, and constitutes material wastefulness.

Unfortunately, the extremely high temperatures reached inside the plasma makes it difficult to perform simple measurements (such as temperature and flow rate) inside the torch. Computational

models offer a facile method for investigating the physical and chemical properties of an ICP and present useful tools for diagnosing behavioural problems in industrial systems, without having to resort to experimental measurements. Obviously, models have to be verified experimentally; they are nevertheless essential for interpreting any measurement made.

There are several existing computational models in the literature. Boulos [3] was the first to develop a computational model for an ICP. Several elementary models followed, focusing on investigating the temperature and flow fields [4-6]. Contemporary models use finite element/volume method software packages and these software suites come with built-in facilities for performing temperature and flow field calculations. Examples of such packages include COMSOL [7] Multiphysics and ANSYS Fluent [8]. For example, Ikhlef *et al*. [9] developed a FEM COMSOL model for an ICP at atmospheric pressure with argon gas using a resistive magnetohydrodynamic model. There are several modern models using FEM or FVM to study different cases or uses of the ICP [10-13]. To the best of our knowledge, none of these takes into account the effect of sheath gas composition.

The aim of this research is the determination of the optimum sheath gas composition such that the energy loss through the sidewall is kept to a minimum. The modelling and simulation was done in COMSOL Multiphysics, using the built-in computational modules. No additional code was written and no experimental measurements are reported here.

2. Computational model

2.1 *Constitutive equations*

Boulos *et al.* [14] developed a mathematical model for the heat of powders in an ICP under dense loading conditions. This model is employed by the COMSOL package. The model is described in the subsequent paragraphs.

The laminar compressible flow in the system is described by the continuity equation and the momentum equation, shown in equation 1 and equation 2, respectively.

$$\nabla \cdot (\rho \boldsymbol{u}) = 0 \tag{1}$$

$$\rho(\boldsymbol{u} \cdot \nabla)\boldsymbol{u} = \nabla \cdot \left[-p\mathbf{I} + \mu\left(\nabla \boldsymbol{u} + (\nabla \boldsymbol{u})^T\right) - \frac{2}{3}\mu(\nabla \cdot \boldsymbol{u})\mathbf{I} \right] + \boldsymbol{F} \tag{2}$$

Here ρ and $\boldsymbol{u}$ are the density and the velocity field, respectively. $\boldsymbol{F}$ is the body force vector, which accounts for all the forces in the volume, inclusive of gravity, electric- and magnetic fields. T, μ, and p are the temperature, viscosity, and pressure, respectively.

The total heat transfer is described by equation 3 and the conductive heat flux described by equation 4.

$$\rho C_p \frac{\partial T}{\partial t} + \rho C_p \boldsymbol{u} \cdot \nabla T + \nabla \cdot \boldsymbol{q} = Q + Q_p + Q_{vd} \tag{3}$$

$$\boldsymbol{q} = -k\nabla T \tag{4}$$

Here Q, Q_p, Q_{vd}, $\boldsymbol{q}$, C_p, and k are the plasma heat source, the pressure work, the viscous dissipation, the conductive heat flux, the specific heat of the gas, and the thermal conductivity of the gas [7], respectively. The Maxwell equations are given in equation 5 to equation 8.

$$\nabla \times \boldsymbol{H} = \boldsymbol{J} \tag{5}$$

$$\boldsymbol{B} = \nabla \times \boldsymbol{A} \tag{6}$$

$$\boldsymbol{J} = \sigma \boldsymbol{E} + j\omega \boldsymbol{D} + \sigma \boldsymbol{v} \times \boldsymbol{B} + \boldsymbol{J_e} \tag{7}$$

$$\boldsymbol{E} = -j\omega \boldsymbol{A} \tag{8}$$

Here $\boldsymbol{H}$, $\boldsymbol{J}$, $\boldsymbol{B}$, $\boldsymbol{A}$, $\boldsymbol{E}$, ω, $\boldsymbol{D}$, $\boldsymbol{J_e}$, σ, and $\boldsymbol{v}$ stand for the magnetic field intensity, current density, magnetic flux density, magnetic vector potential, electric field intensity, frequency, electric displacement, externally generated current density, electrical conductivity, and velocity of the geometry relative to the reference system, respectively.

The plasma heat source Q, used in equation 3, is defined by equation 9.

$$Q = \frac{\partial}{\partial T}\left(\frac{5k_B T}{2q}\right)(\nabla T \cdot \boldsymbol{J}) + (\boldsymbol{E} \cdot \boldsymbol{J}) + Q_{rad} \tag{9}$$

Here k_B, q, and Q_{rad} are the Boltzmann constant, the unit charge, and the total volumetric emission loss, respectively. The first term on the right-hand side represents the enthalpy transport. The second term accounts for Joule heating.

2.2 *Computational Modelling*

The mathematical model, presented in equations 1 to 9, was used to simulate the Tekna torch system using COMSOL Multiphysics. The model was implemented *via* three physics nodes *viz.* fluid dynamics, heat transfer and the electromagnetic field. The magnetic field node solves the Maxwell equations for the electromagnetic fields produced due to an alternating current in the coil. The COMSOL plasma package was used to interface the magnetic field node and the heat transfer node, providing the plasma heat source. Laminar flow, optically thin plasma, and local thermodynamic equilibrium was assumed.

The model geometry is presented in figure 2. This geometry is a practical simplification of the technical schematic. Since the torch exhibits cylindrical symmetry, the geometry was simplified to permit 2D axisymmetric simulation, significantly cutting down on required computational resources and decreasing the simulation time.

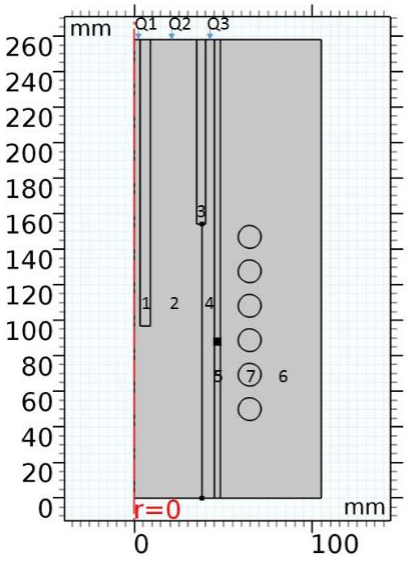

Figure 1. Simulated geometry indicating different domains and inlets.

Domain 1 (in figure 2) is the wall of the carrier gas probe and Q1 is the carrier gas inlet. Domain 2 is the central plasma gas, domain 3 the quartz tube separating the plasma gas and the sheath gas. Domain 4 is the sheath gas and domain 5 the torch wall. The fluid dynamic equations were only solved over domain 2 and 4 with a no-slip boundary condition on the torch sidewall (the boundary between Domain 4 and 5). The boundary between Domain 2 and 4 is open with no physical effects on the flow and heat transfer.

COMSOL does not properly account for the mixing of gases in a plasma. Modelling a system with hydrogen in the sheath gas and pure argon in the main plasma gas requires one to trick the software with a *faux* partition to produce two separate regions with dissimilar composition, while still

permitting the unified treatment of heat transfer and flow. Domain 4 is, therefore, a homogenous mixture of hydrogen and argon and the properties of this mixture programmed manually.

The heat transfer was determined in Domains 2, 4, and 5. The heat transfer in the rest of the geometry was regarded as of no concern since the heat is lost through the cooling water which is included in the model through a fixed temperature boundary condition of 300 K on the outside wall. The initial temperature was set to 300 K for the entire geometry and the initial velocity field was set to 0 m/s.

The system was studied in a frequency-transient domain for 30 s of operating time. 5 simulations were run at varying amounts of H_2 in the sheath gas (0 vol%, 5 vol%, 7.5 vol%, 10 vol% and 50 vol%). Table 1 shows the operating conditions and initial values kept constant for all the simulations.

Table 1. Operating conditions and initial values.

Property	Value	Unit
Power	11	kW
Frequency	3	MHz
Inlet 1 (Q1)	2	slpm
Inlet 2 (Q2)	10	slpm
Inlet 3 (Q3)	40+*x*	slpm
Initial temperature	300	K
Initial flow field	0	m/s
Initial magnetic vector potential	0	Wb/m
Pressure	85	kPaa

3. Results and discussion

The main results are provided graphically in figure 4 to figure 8. Figure 3 graphs the electrical conductivity of hydrogen and argon as a function of temperature, as used by COMSOL. In the temperature range of interest, *viz.*, 5 000 K to ~ 20 000K, the electrical conductivity of argon is higher than hydrogen and will, therefore, ionize more easily and at lower temperatures than hydrogen. This is due to the fact that in the case of hydrogen energy goes into both bond breaking and ionization. Figure 4 shows the temperature at a fixed point in the centre of the sidewall. This point was set at the height where the maximum temperature was achieved in each simulation. Figure 5 shows the temperature 1 mm away from the torch sidewall. Figure 6 shows the total normal heat flux across the boundary on the outer sidewall. Figure 7 shows the temperature profile of the geometry at 0 vol%, 10 vol% and 50 vol% H_2. Figure 8 shows the radial temperature profile at the maximum temperature for each simulation case.

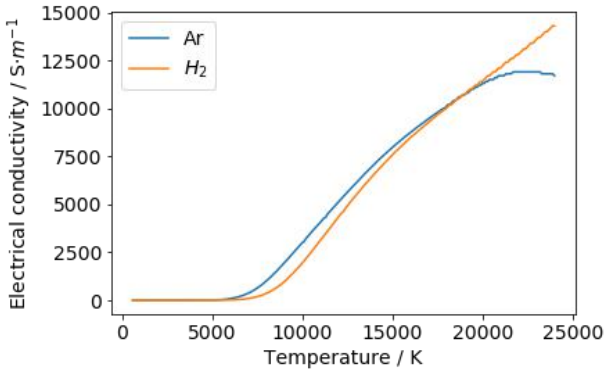

Figure 2. Electrical conductivity of argon and hydrogen gas as a function of temperature [14].

The time-dependent temperature (figure 4) calculated for the sidewall appears to reach a steady-state after about 20 s. Therefore all simulations were run for a total of 30 s. The maximum Reynolds number over the whole geometry was found to be 18.97, indicating the assumption of laminar flow to be correct.

It should be noted that the 0.0 vol% H_2 and 7.5 vol% H_2 lines overlap. The presence of hydrogen moves the heated zone to the left and reduces plasma formation near the torch wall (as shown in figure 6 and figure 7); however, it also increases heat transfer to the torch sidewall. This is expected as hydrogen exhibits a greater thermal conductivity than argon. The overlap implies that the mitigation of heat loss to the reactor walls essentially becomes a trade-off between the effects of improved heat transfer to the wall, the increasing distance of the hot zone from the wall due to reduced plasma formation and the energy loss to H-H bond dissociation.

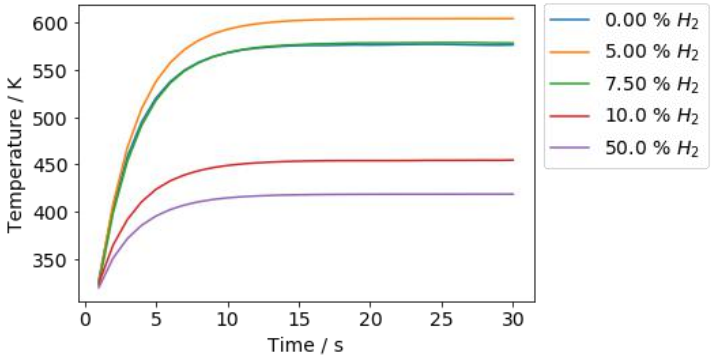

Figure 3. Temperature in the centre of the torch sidewall at the height of the maximum

Figure 5 shows the temperature 1 mm away from the torch sidewall over the full torch length for different concentrations H_2 in the sheath gas at the final time step. Above 5 vol% H_2 in the sheath gas, the maximum temperature is below 5000 K. This is the temperature at which argon begins to ionize. The implication is that no plasma formation occurs at the torch sidewall. Figure 6 shows the total normal heat flux across the boundary on the outer sidewall for the different concentrations of H_2 gas. Table 2 shows the total power lost through the torch side wall for each case.

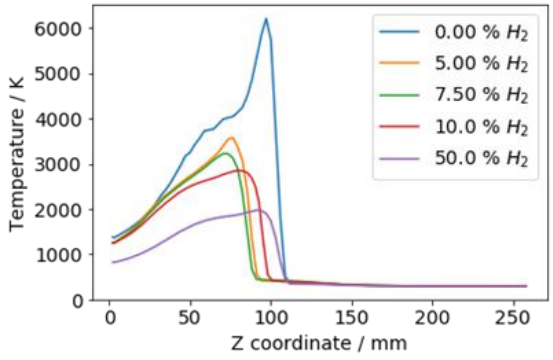

Figure 4. Temperature 1 mm from the torch sidewall for different concentrations of H_2 in the sheath gas.

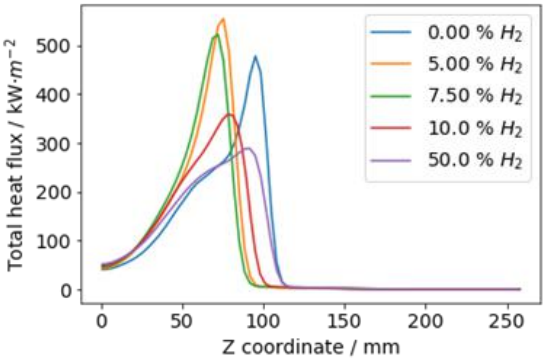

Figure 5. Total heat flux across the boundary at the outer sidewall of the torch at different concentrations of H_2 gas.

Table 2. Total power lost through torch outside wall

Percentage H_2 in sheath gas	Total heat lost
0	6.37 kW
5	6.08 kW
7.5	5.91 kW
10	5.64 kW
50	5.73 kW

Figure 7 shows the temperature profile of the geometry at 0 vol%, 10 vol% and 50 vol% H_2 to indicate how the heated zone has moved to the left with the increased H_2 gas in the sheath.

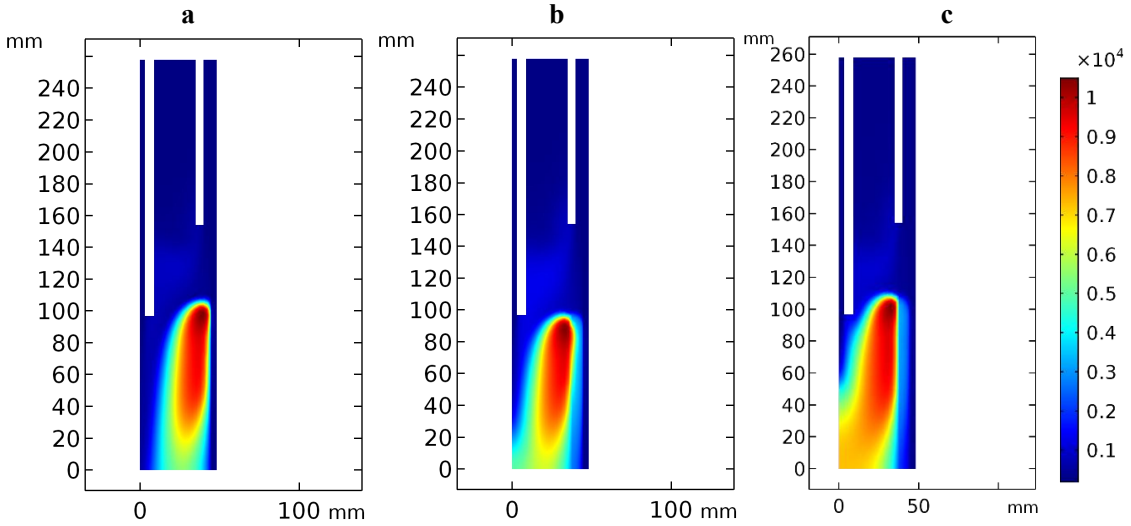

Figure 6. Temperature profile with: a) 0 vol%, b) 10 vol% and c) 50 vol% H2 in the sheath gas.

The absence of data in Figure 8 in the 0 vol% and 50 vol% H_2 line is due to the heated zone being higher in the geometry so the radial profile passes through the carrier gas probe where the heat transfer was not solved.

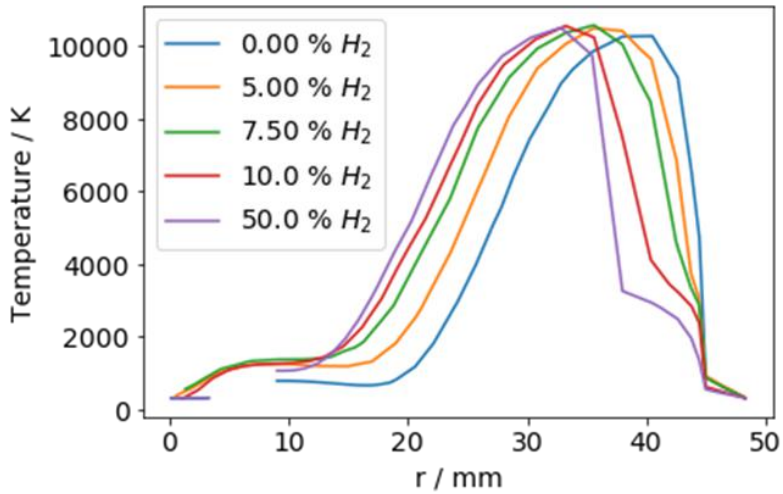

Figure 7. Radial temperature profile at the maximum temperature.

Hydrogen in the sheath gas clearly reduces the temperature at the torch sidewall and results in less heat lost through the sidewall. The temperature on the inside wall reaches a maximum of 914 K with 7.5 vol% H2 in the sheath gas. This is a low enough temperature to prevent thermal damage to the torch and still have a minimal effect on the plasma and energy costs. Less than 7.5 vol% H2 causes an increased temperature in the wall due to the increased heat transfer capability of hydrogen. The total energy loss appears to reach a minimum at 10 vol% H2. The sheath gas composition for minimum energy loss seems to be between 7.5 vol% and 10 vol% H2.

4. Conclusion

The computational model indicates that isolating the side wall of an ICP torch from the plasma with a hydrogen/argon sheath gas reduces the energy lost through the wall. Hydrogen increases the sheath gas heat transfer capability but shifts the plasma away from the side wall. These two competing

mechanisms result in a minimum energy loss when the sheath gas hydrogen content ranges between 7.5 and 10 vol%. If the hydrogen content is below 7.5 vol%, more energy is lost to the side wall than with a pure argon sheath gas. The more computational effort is required to determine the exact composition of the sheath gas needed to achieve minimum energy loss.

References

[1] Murr LE, Martinez E, Amato KN, Gaytan SM, Hernandez J, Ramirez DA, Shindo PW, Medina F, and Wicker RB 2012 Fabrication of Metal and Alloy Components by Additive Manufacturing: Examples of 3D Materials Science *J. Mater. Res. Technol.* **1** 42
[2] Tekna 2016 Tekna Spheroidization system Teksohero-15 system http://www.tekna.com/landing-page/teksphero-15 [16 July 2018]
[3] Boulos MI 1978 Heating of Powders in The Fire Ball of an Induction Plasma *IEEE Trans. Plasma Sci*. **6** 93
[4] Proulx P, Mostaghimi J and Boulos MI 1983 *Int. J. Heat Mass Transfer.* **28** 1327
[5] Mostaghimi J, Proulx P and Boulos MI 1985 Computer modeling of the emission patterns for a spectrochemical ICP *Numer. Heat Tran* **8** 187
[6] Yang P, Barnes RM, Mostaghimi J and Boulos MI 1989 Application of a two-dimensional model in the simulation of an analytical inductively coupled plasma discharge *Spectrochim. Acta, Part B* **44** 657
[7] COMSOL 2018 COMSOL Multiphysics 5.3a https://www.comsol.com/ [16 July 2018]
[8] Ansys 2018 Ansys Fluent https://www.ansys.com/products/fluids/ansys-fluent [16 July 2018]
[9] Ikhlef N, Hacib1 T, Leroy O, and Mékiddèche MR 2012 Nonlinear compressible magnetohydrodynamic flows modeling of a process ICP torch *Eur. Phys. J. Appl. Phys*. **58** 10804
[10] Aghaei M and Bogaerts A 2016 Particle transport through an inductively coupled plasma torch: elemental droplet evaporation *J. Anal. At. Spectrom.* **31** 631
[11] Bolot R, Coddet C, Schreuders C, Leparaoux M and Siegmann S 2007 Modeling of an Inductively Coupled Plasma for the Synthesis of Nanoparticles *J. Therm Spray Technol.* **16** 690
[12] Bogaerts A and Aghaei M 2017 Inductively coupled plasma-mass spectrometry: insights through computer modeling *J. Anal. At. Spectrom.*, **32**, 203
[13] Colombo V, Ghedini E and Mostaghimi J 2008 Three-Dimensional Modeling of an Inductively Coupled Plasma Torch for Spectroscopic Analysis *IEEE Trans. Plasma Sci.* **36** 1040
[14] Boulos MI, Fauchais P and Pfender E 1994 Plasma tables *Thermal Plasmas: Fundamentals and Applications* (New York: Plenum Press) Appendix A.3 pp 388-447